Published in final edited form as:
J Immunol. 2012 August 15; 189(4): 1937–1945. doi:10.4049/jimmunol.1200658.

CD8 T cell-initiated blood brain barrier disruption is independent of neutrophil support

Holly L. Johnson[*,†,‡], **Yi Chen**[§], **Fang Jin**[†], **Lisa M. Hanson**[†], **Jeffrey D. Gamez**[*], **Istvan Pirko**[*], and **Aaron J. Johnson**[*,†]

[*]Department of Neurology, Mayo Clinic, Rochester, Minnesota

[†]Department of Immunology, Mayo Clinic, Rochester, Minnesota

[‡]Neurobiology of Disease Graduate Program, Mayo Graduate School, Rochester, Minnesota

[§]Department of Neurology, University of Cincinnati, Cincinnati, Ohio

Abstract

Blood brain barrier (BBB) disruption is a common feature of numerous neurologic disorders. A fundamental question in these diseases is the extent inflammatory immune cells contribute to CNS vascular permeability. We have previously shown that CD8 T cells play a critical role in initiating BBB disruption in the peptide induced fatal syndrome (PIFS) model developed by our laboratory. However, myelomonocytic cells such as neutrophils have also been implicated in promoting CNS vascular permeability and functional deficit in murine models of neuroinflammatory disease. For this reason, we evaluated neutrophil depletion in a murine model of CD8 T cell-initiated BBB disruption by employing traditionally used anti-GR-1 monoclonal antibody (mAb) RB6-8C5 and Ly-6G-specific mAb 1A8. We report that CNS-infiltrating antiviral CD8 T cells express high levels of GR-1 protein and are depleted by treatment with RB6-8C5. Mice treated with RB6-8C5, but not 1A8, display: 1.) intact BBB tight junction proteins, 2.) reduced CNS vascular permeability visible by gadolinium enhanced T1 weighted MRI, and 3.) preservation of motor function. These studies demonstrate that traditional methods of neutrophil depletion with RB6-8C5 are broadly immune-ablating. Our data also provide evidence that CD8 T cells initiate disruption of BBB tight junction proteins and CNS vascular permeability in the absence of neutrophil support.

Introduction

Blood brain barrier (BBB) disruption is an integral feature of severe neurological disorders, including multiple sclerosis (MS), acute hemorrhagic leukoencephalitis (AHLE), stroke, dengue hemorrhagic fever, and cerebral malaria (1–7). A fundamental question in these diseases is the extent inflammatory immune cells contribute to CNS vascular permeability. This lack of understanding currently undermines the development of more focused therapeutic approaches to ameliorate pathology associated with BBB disruption. Several experimental model systems have proposed roles for different immune cell types in contributing to CNS vascular permeability. CD4 T cells have been demonstrated to initiate BBB disruption in experimental autoimmune encephalomyelitis (EAE) by inducing astrocytes to release vascular endothelial growth factor (VEGF), ultimately leading to alterations in the tight junction architecture and ensuing CNS vascular permeability (8). Other studies using lipopolysaccharide (LPS) injection have investigated the capacity of

Correspondence address: Dr. Aaron J. Johnson, Mayo Clinic Department of Immunology, Guggenheim 411C, 200 First Street SW, Rochester, MN 55905. Phone: 507-266-1973 Fax: 507-284-1637 Johnson.Aaron2@mayo.edu.

TNF-α to mediate reactive microgliosis and tight junction protein alterations, leading to BBB disruption (9, 10). Finally, studies involving lymphocytic choriomeningitis virus (LCMV) infection have proposed a role for both CD8 T cells and myelomonocytic cells such as neutrophils in initiating BBB disruption (11–14). Therefore, how lymphocytes and innate immune cells interact to promote BBB disruption is critical to our understanding of immune-mediated BBB permeability.

Our laboratory has developed a novel mouse model of CNS vascular permeability using a variation of the Theiler's murine encephalomyelitis virus (TMEV) model of multiple sclerosis (15–17). Seven days after intracranial TMEV infection, C57BL/6 mice mount an antiviral CD8 T cell response that is highly focused on the immunodominant TMEV peptide, $VP2_{121\text{-}130}$, presented in the context of the D^b class I molecule (18, 19). Injection of this $VP2_{121\text{-}130}$ peptide 7 days post-TMEV infection, during the expansion of D^b:$VP2_{121\text{-}130}$ epitope-specific CD8 T cells, results in severe CNS vascular permeability and death within 48 hours (15). No vascular permeability or overt pathology is observed in organs outside of the CNS (20). Meanwhile, magnetic resonance imaging (MRI) analysis reveals areas of microhemorrhages, edema, and tissue damage in the brains of these mice (6). This peptide induced fatal syndrome (PIFS) is therefore a readily inducible model system to investigate CD8 T cell-initiated CNS vascular permeability. PIFS resembles features of human acute hemorrhagic leukoencephalitis (AHLE) and enables the study of how CNS vascular permeability is mediated in hemorrhagic infections and hemorrhagic demyelinating conditions (6, 21, 22). We have also demonstrated that other immune cells implicated in promoting BBB disruption, such as CD4 T cells and cytokines such as TNF-α, do not contribute to morbidity and mortality in the PIFS model (15).

In accordance with our work using the PIFS model system, CD8 T cells have also been implicated in contributing to BBB disruption and hemorrhage formation in an experimental model of cerebral malaria (7). Furthermore, studies using the lymphocytic choriomeningitis virus (LCMV) model have demonstrated the importance of CD8 T cells in contributing to mortality in model systems characterized by CNS vascular permeability (11–14). However, myelomonocytic cells, which encompass monocytes and neutrophils, were perceived to be the critical cell type promoting vascular permeability associated with CD8 T cell-dependent morbidity. This conclusion was based on the results of neutrophil depletion with anti-granulocyte receptor-1 (GR-1) monoclonal antibody (mAb) RB6-8C5, a widely used method to evaluate the role of neutrophils in several disease processes, including cancer (23, 24). Using this approach, it was proposed that CD8 T cells may primarily serve to attract other effector populations such as neutrophils to induce BBB disruption (13). However, RB6-8C5 has been shown to be non-specific for neutrophils, as it binds to both Ly-6G on neutrophils and Ly-6C on lymphocytes and monocytes (25, 26). RB6-8C5 has also been shown to bind to F4/80 macrophages/monocytes, plasmacytoid dendritic cells, and CD8 T cells in a model of herpes simplex virus type 1 infection (27). Consequently, it is possible that this antibody is also ablating activated CD8 T cells, which we have previously shown to be critical for initiating BBB disruption (6, 15, 20, 28). We have also demonstrated that depletion of antigen-specific CD8 T cells confers protection (15). Therefore, due to the lack of specificity of the broadly used mAb RB6-8C5, it is essential to reassess the capacity of neutrophils to contribute to BBB disruption in models of neurological diseases. In this study, we employed both anti-GR-1 mAb RB6-8C5 and anti-Ly-6G mAb 1A8 to deplete neutrophils in vivo (25–27, 29). We investigated the impact of these neutrophil depletion strategies on brain-infiltrating CD8 T cell populations, BBB tight junction protein alterations, CNS vascular permeability, and functional deficit using the PIFS model system.

Materials and Methods

Animals

C57BL/6 male mice were obtained from Jackson laboratories (Bar Harbor, ME) at 6 weeks of age. All experiments were approved by the Institutional Animal Care and Use Committee of the University of Cincinnati and Mayo Clinic.

Induction of CNS vascular permeability using the PIFS model

CNS vascular permeability was induced as previously described (15, 20, 28). Briefly, all mice were intracranially infected with 2×10^6 PFU Daniel's strain of TMEV. Seven days later, during the peak of CD8 T cell expansion in the brain, mice were intravenously administered 0.1 mg $VP2_{121\text{-}130}$ (FHAGSLLVFM) peptide or mock control E7 (RAHYNIVTF) peptide (Genescript) (15).

Neutrophil depletion strategies

Mice were administered either 250 μg anti-GR-1 mAb RB6-8C5 (BioXCell, #BE0075), 500 μg anti-Ly-6G mAB 1A8 (BioXCell, #BE0075-1), or 500 μg normal rat serum (Jackson, #89531) on days 5, 6, and 7 post-TMEV infection.

Rotarod

Mice were placed on the Rotamex-5 rotarod apparatus (Columbus Instruments) increasing from 5–40 RPMs over 7 minutes to evaluate functional deficit. The motor performance of mice was assessed before and after the induction of CNS vascular permeability, and the scores are depicted as percent initial motor ability (28).

Injection of FITC-albumin to assess permeability

Mice were given an intravenous injection of 10 mg FITC-albumin (Sigma #A9771) 23 hours after $VP2_{121\text{-}130}$ or E7 peptide administration, and brains were harvested at 24 hours.

Flow Cytometry

The left hemisphere was strained through a nylon mesh 100 μm filter into RPMI, and 700 μg of collagenase type IV (Worthington) was added to each 5-ml tissue suspension. Suspensions were then incubated in a 42°C water bath for 45 minutes. Each suspension was then added to a solution containing 1 ml 10× PBS, 9 ml percoll, and 10 ml RPMI and spun at 7840 × g for 30 minutes. A lymphocyte layer present in the bottom 10 ml of solution was collected and diluted with RPMI to a total volume of 50 ml. Cell suspensions were then spun at 300 × g for 10 minutes. Media was aspirated off and cell pellet was resuspended in RPMI. Isolated brain lymphocytes were washed twice with FACS buffer and then incubated with the following antibodies for 40 minutes: D^b:$VP2_{121\text{-}130}$ tetramer APC, anti-GR-1 FITC, anti-Ly-6G biotin, and anti-CD45 PerCP. This was followed by a 20 minute incubation with anti-CD8 PE-Cy7. Cells were washed twice with FACS buffer and then incubated for 20 minutes with PE streptavidin. Cells were once again washed twice with FACS buffer and then fixed in 4% paraformaldehyde and 1× PBS. Samples were analyzed on a BD LSRII flow cytometer (BD Biosciences) using FACS Diva software (BD Biosciences).

Cell Sorting

Ly-6G+ cells were sorted using an EasySep negative selection kit (Stemcell Technologies, #19753). Isolated CNS-infiltrating lymphocytes were suspended in PBS, 2% FBS, and NRS at a concentration of 1×10^8 cells/ml. Cells were then stained with anti-Ly6G biotin and incubated with biotin cocktail (100 μl/mL) for 15 minutes. Magnetic nanoparticles were

then added at 50 μl/ml cells and incubated for 15 minutes. The cell suspension was brought to a total volume of 2.5 ml by adding PBS + 2% FBS. The tube containing this cell suspension was then placed in an EasySep magnet (Stemcell Technologies, #19753) for 5 minutes. The magnet was then inverted into a new tube. A Wright-Giemsa stain and cytospin analysis were used to visualize Ly-6G+ cells.

Confocal Microscopy

Fresh frozen coronal slices from FITC-albumin injected mice were cut on a cryostat and placed onto positively charged slides. Slides were washed twice with PBS and then fixed in 3% paraformaldehyde for 15 minutes. Slides were then rinsed three times in PBS, followed by a 1 hour incubation in 5% normal goat serum + 0.5% Igepal CA-630 (Sigma I3021) in PBS. Slides were incubated with the following primary antibodies at a concentration of 1:250 overnight at room temperature: mouse anti-claudin-5 (Invitrogen, 35–2500) and rabbit anti-occludin (Invitrogen, 71–1500). Slides were then rinsed 5 times in PBS. The following secondary antibodies were then added at a concentration of 1:250 for 1 hour at room temperature: AlexaFluor 532 goat anti-mouse IgG (H+L) (Invitrogen, A-11002) and AlexaFluor 647 goat anti-rabbit IgG (H+L) (Invitrogen, A-21244). Slides were rinsed 5 times in PBS followed by Hoechst staining at a concentration of 1:500 in PBS for 5 minutes. Slides were then rinsed 5 times in PBS, dried, and covered with Vectashield medium (Vector lab, H-1000). Images were acquired using a Leica (Germany) DM 2500 confocal microscope equipped with a 63× oil immersion objective (numerical aperture 1.30). All images were collected at room temperature using Type F immersion liquid (Leica Microsystems) and analyzed using LAS AF stimulator AF 6000 acquisition software.

MRI Acquisition

A Bruker Avance II 7 Tesla vertical bore small animal MRI system (Bruker Biospin) was used for image acquisition to evaluate CNS vascular permeability. Image acquisition was performed as previously described (6, 30). Briefly, inhalation anesthesia was induced and maintained via 3–4% isoflurane. Respiratory rate was monitored during the acquisition sessions using an MRI compatible vital sign monitoring system (Model 1030, SA Instruments, Inc., Stony Brook, NY). Mice were given an intraperitoneal (i.p.) injection of gadolinium using weight based dosing of 100 mg/kg, and after a standard delay of 15 minutes, a volume acquisition T1 weighted spin echo sequence was used (TR=150 ms, TE=8 ms, FOV: 32 mm × 19.2 mm × 19.2 mm, Matrix: 160 × 96 × 96, number of averages=1) to obtain T1 weighted images.

Image Analysis

3D volumetry was performed as previously described (31–33). Briefly, the 3D volume of vascular permeability was quantified using Analyze 10 software (Biomedical Imaging Resource, Mayo Clinic). Brains from the gadolinium enhanced T1 weighted images were extracted using the 3D volume extractor tool. The 3D ROI tool was used to define areas of gadolinium leakage using semi-automated methods, including a combination of thresholding and seed growing tools. The identified volume of gadolinium enhancement was saved as a 3D object designating a subvolume of the brain. The 3D sampling tool was then used to calculate the actual volume of this object, which corresponds with the volume of gadolinium leakage in the studied brain. To generate figures, 3D object rendering using the volume rendering tool was performed to visualize the identified volumes of contrast enhancement.

Statistical Analysis

Mean and standard error values were calculated using SigmaStat software (SYSTAT Software Inc). GraphPad Prism Software was used to construct bar graphs with standard

error bars. A Student's t-test was performed using SigmaStat to evaluate the extent CD8 T cells bind to GR-1+ or Ly-6G+ protein and also to assess the efficacy of neutrophil depletion. A Mann-Whitney Rank Sum test was performed using SigmaStat to evaluate total numbers of GR-1+ or Ly-6G+ cells. An analysis of variance (ANOVA) followed by a test for pairwise multiple comparisons (Tukey's test or Dunn's method) using SigmaStat was employed to determine significance between the three treatment groups with regards to ablation of CD8 T cells, quantification of the 3D volume of CNS vascular permeability, and rotarod scores.

Results

The anti-granulocyte receptor-1 (GR-1) mAb RB6-8C5 binds to CD8+ cells

CNS-infiltrating lymphocytes isolated from TMEV-infected C57BL/6 mice that received $VP2_{121-130}$ peptide to induce PIFS (n=8) were stained with antibody to GR-1, Ly-6G, CD45, CD8, and D^b:$VP2_{121-130}$ tetramer. We found that the vast majority (94.9%) of brain-infiltrating CD8 T cells also stained positive for GR-1 protein when compared to the percentage of Ly-6G+ CD8+ cells ($p<0.001$) (Figure 1A–1D). Additionally, we found that CNS-infiltrating D^b:$VP2_{121-130}$ epitope-specific CD8+ cells isolated from C57BL/6 mice induced to undergo PIFS (n=8) had significantly higher GR-1 protein expression (95.7% ± 0.314) when compared to CD8+ cells isolated from the spleen of uninfected (10.4% ± 0.819) (n=3) ($p<0.001$) or intracranially TMEV-infected (25.4% ± 3.901) (n=6) ($p<0.001$) C57BL/6 mice. These results demonstrate that peripheral CD8 T cells do not express GR-1 protein at the level of activated CNS-infiltrating antiviral CD8 T cells (Figure 1E). Percentages are depicted as mean ± SEM. In addition, we performed a magnetic Ly-6G+ sort (see methods) to visualize brain-infiltrating Ly-6G+ cells and determined these cells have morphological features characteristic of neutrophils (i.e. segmented nuclei) (Figure 1F). This observation is in accordance with previously published reports that anti-Ly-6G mAb 1A8 is highly specific for neutrophils. (25–27, 29). Furthermore, we evaluated GR-1 positivity on other brain-infiltrating cells and found that the vast majority of CD3+, CD11c +, and Mac-1+ cells also stained positive for GR-1 protein. Approximately half of CD4+ cells and a quarter of NK1.1+ cells were also positive for GR-1 protein (n=4) (Figure 1G–1K).

Efficacy of mAb RB6-8C5 and 1A8 neutrophil depletion strategies during acute TMEV infection

With the observation that GR-1 protein was highly expressed on CNS-infiltrating CD8 T cells, we next assessed the efficacy of our neutrophil depletion strategies using anti-GR-1 mAb RB6-8C5 and anti-Ly-6G mAb 1A8 during acute TMEV infection. We performed flow cytometric analysis of lymphocytes isolated from the brains of C57BL/6 mice intraperitoneally (i.p.) administered normal rat serum (NRS) (n=6), anti-GR-1 mAb RB6-8C5 (n=6), or anti-Ly-6G mAb 1A8 (n=6). Isolated CNS-infiltrating lymphocytes were then stained with antibody to GR-1, Ly-6G, CD45, CD8, and D^b:$VP2_{121–130}$ tetramer. We determined that i.p. administered mAb RB6-8C5 significantly depleted GR-1+ cells as a percentage of $CD45^{hi}$ cells (Figure 2B) ($p<0.001$) and mAb 1A8 significantly depleted Ly-6G+ cells as a percentage of $CD45^{hi}$ cells (Figure 2F) ($p=0.008$) when compared to the levels of these cells in mice treated with normal rat serum (Figure 2A and 2D). We also analyzed absolute numbers of GR-1+ or Ly-6G+ cells per 100,000 events and found that treatment with mAb RB6-8C5 significantly depleted GR-1+ cells (Figure 2G) ($p=0.004$) and mAb 1A8 significantly depleted Ly-6G+ cells (Figure 2H) ($p=0.002$) when compared to treatment with normal rat serum. Additionally, we used IgG2b as an isotype control for mAb RB6-8C5 and IgG2a as an isotype control for mAb 1A8. Treatment with IgG2b (n=3) did not significantly affect the percentage of GR-1+ cells when compared to treatment with

normal rat serum (p=0.935). Similarly, treatment with IgG2a (n=3) also did not significantly affect the percentage of Ly-6G+ cells when compared to treatment with normal rat serum (p=0.400) (data not shown). Additionally, we determined that RB6-8C5 is broadly immune-ablating, in that we observed significant reduction of CD45+ cells as a percentage of whole brain cells when compared to positive controls treated with normal rat serum (p=0.009) (Figure 2I).

The anti-granulocyte receptor-1 (GR-1) mAb RB6-8C5 depletes CNS-infiltrating CD8+ cells in mice administered $VP2_{121-130}$ peptide to induce PIFS

The above experiments prompted the question of whether treatment with RB6-8C5 would also cause ablation of virus-specific CD8 T cells in addition to neutrophils. In order to address this, isolated CNS-infiltrating lymphocytes from C57BL/6 mice treated with normal rat serum (n=6), anti-GR-1 mAb RB6-8C5 (n=6), or anti-Ly-6G mAb 1A8 (n=6) were stained with antibody to GR-1, Ly-6G, CD45, CD8, and D^b:$VP2_{121-130}$ tetramer. Figure 3A–3D illustrates that treatment with RB6-8C5 resulted in a significant reduction in CNS-infiltrating CD8 T cells as a percentage of CD45+ cells when compared to treatment with normal rat serum ($p<0.05$) or treatment with the more neutrophil-specific mAb 1A8 ($p<0.05$). Additionally, mock treatment with IgG2b and IgG2a isotype controls did not affect the percentage of CD8+CD45+ cells when compared to treatment with normal rat serum (data not shown). Taking into account that RB6-8C5 treatment also resulted in an overall loss of CD45+ cells (Figure 2G), we also analyzed the reduction in overall CD8 T cell numbers. Treatment with RB6-8C5 therefore significantly reduces the total number of CD8+ cells per 100,000 events when compared to treatment with normal rat serum and isotype-matched controls (Figure 3E) ($p<0.05$).

Neutrophil depletion with mAb 1A8 does not preserve BBB tight junctions in CD8 T cell-initiated BBB disruption

We have previously shown that CD8 T cells initiate BBB tight junction protein alterations in microvessels and CNS vascular permeability in the PIFS model of CD8 T cell-initiated BBB disruption (28). We therefore evaluated the effect of neutrophils and CD8 T cells on vascular integrity and the tight junction architecture in animals induced to undergo PIFS through administration of $VP2_{121-130}$ peptide. Administration of mock human papilloma virus E7 peptide was used as a negative control, as this peptide does not induce PIFS (6, 15, 20, 28) (Figure 4A). Treatment with anti-GR-1 mAb RB6-8C5 (Figure 4C) preserved BBB tight junction proteins and vascular integrity similar to that observed in negative controls. However, treatment with normal rat serum (Figure 4B) or neutrophil-ablating Ly-6G mAb 1A8 (Figure 4D) resulted in loss of the BBB tight junction proteins claudin-5 and occludin in areas of vascular permeability. Through extensive analysis of numerous areas of vascular permeability, we found that leakage of FITC-albumin coincided with disruption of tight junction proteins in 15 out of 15 areas for mice treated with normal rat serum, and 12 out of 12 areas for mice treated with 1A8. This correlation is consistent with BBB tight junction protein disruption co-localizing with vascular permeability. Therefore, CD8 T cell-initiated disruption of BBB tight junction proteins and ensuing CNS vascular permeability are not dependent on the contribution of neutrophils.

Neutrophil depletion with mAb 1A8 does not preserve vascular integrity as measured by 3D volumetric analysis of gadolinium enhancement visible on T1 weighted MRI

Our analysis using confocal microscopy demonstrated that CD8 T cell-initiated vascular permeability co-localized with BBB tight junction protein degradation. To quantitatively determine the full volume of CNS vascular leakage in animals undergoing CD8 T cell-initiated BBB disruption, we employed volumetric analysis of 3D gadolinium enhanced MRI. Because neutrophils have been strongly implicated in promoting CNS vascular

permeability (13, 34, 35), we sought to determine the extent neutrophils were contributing to CD8 T cell-initiated BBB disruption. To accomplish this, we conducted gadolinium enhanced T1 weighted MRI to measure vascular permeability following neutrophil depletion strategies using anti-GR-1 mAb RB6-8C5 and Ly-6G-specific mAb 1A8, 24 hours post-induction of PIFS with administration of $VP2_{121-130}$ peptide. The extent gadolinium leaked into the CNS was quantified using 3D volumetric analysis with Analyze 10 software developed by Mayo Clinic's Biomedical Imaging Resource (36, 37). Quantification of the 3D volume of gadolinium leakage from vasculature (Figure 5I) revealed that treatment with RB6-8C5, which we have also shown to deplete CD8 T cells (Figure 3B and 3D), was effective at reducing CNS vascular permeability (Figure 5C and 5G) when compared to normal rat serum (Figure 5B and 5F) ($p<0.05$). In contrast, highly neutrophil-specific depletion with mAb 1A8 was not effective at reducing 3D gadolinium leakage (Figure 5D and 5H). As an additional negative control, we evaluated the effect of treatment with isotype-matched antibody on vascular integrity. Treatment with IgG2b (isotype control for RB6-8C5) and IgG2a (isotype control for 1A8) did not significantly affect the extent of CNS vascular permeability when compared to treatment with normal rat serum ($p=0.368$) (data not shown). Therefore, anti-GR-1 treatment with mAb RB6-8C5 is highly effective at protecting from CNS vascular permeability in the PIFS model. Meanwhile, specific ablation of neutrophils with mAb 1A8 did not reduce CNS vascular permeability in this study.

Neutrophil depletion with mAb 1A8 does not preserve functional ability in the PIFS model

In the above experiments, we determined that anti-GR-1 mAb RB6-8C5 causes ablation of CD8 T cells in addition to neutrophils. In contrast, Ly-6G-specific mAb 1A8 is more selective for neutrophils. We next assessed the effect of these treatments on functional deficit by assessing mice on the Rotamex Rotarod before and 24 hours post-induction of PIFS. Seven day TMEV-infected animals were administered $VP2_{121-130}$ peptide to initiate BBB disruption, CNS vascular permeability, and functional deficit (6, 15, 20, 28) As depicted in Figure 6, we determined that treatment with mAb RB6-8C5 significantly preserved motor function when compared to mice treated with normal rat serum or neutrophil-depleting mAb 1A8 ($p<0.05$). These results indicate that functional deficit is dependent on the presence of GR-1+ cells, including CD8 T cells. Meanwhile, consistent with the above data demonstrating a negligible effect of mAb 1A8 on BBB disruption, neutrophil depletion did not affect functional deficit in animals undergoing PIFS.

Discussion

Depletion of neutrophils with anti-GR-1 mAb RB6-8C5 is a widely used method to evaluate the role of neutrophils in several disease processes (13, 23, 24, 34, 38–43). However, this study demonstrates that the use of mAb RB6-8C5 is highly nonspecific. Importantly, activated CNS-infiltrating CD8 T cells express high levels of GR-1 and are depleted by treatment with mAb RB6-8C5. For this reason, previous reports implying a neutrophil subset being required for immune-mediated BBB disruption may require further evaluation before such a conclusion can be drawn (13, 34, 35). Depletion of neutrophils with mAb 1A8, which is highly specific for the neutrophil subset, did not affect CD8 T cell-initiated BBB disruption in these studies.

The extent inflammatory immune cells contribute to CNS vascular permeability in immune-mediated neurological diseases, including multiple sclerosis (MS), acute hemorrhagic leukoencephalitis (AHLE), stroke, dengue hemorrhagic fever, and cerebral malaria, remains largely unknown (1–7). Insult to the CNS results in homing of inflammatory immune cells. However, while these cells are capable of entering the CNS, the BBB remains relatively impermeable to other blood derived products. This may be due to the route immune cells use to gain access to the CNS. Rather than opening tight junctions between cerebral endothelial

cells (CECs) of the vasculature, immune cells enter the CNS via postcapillary venules (44–46). Current models propose a role for inflammatory immune cells in opening tight junctions, resulting in increased permeability of blood derived products (3, 47). Immune cells may also mediate the release of certain chemokines and cytokines, including vascular endothelial growth factor (VEGF), IFN-γ, TNF-α, IL-1β, and IL-6, which may also contribute to increased vascular permeability (8, 20, 22, 48–53).

Studies performed in the various experimental model systems have proposed mechanisms for immune-mediated BBB disruption. The readily inducible PIFS model of CNS vascular permeability developed by our laboratory has enabled us to analyze the kinetics of immune-mediated BBB disruption. We have previously shown that this disruption is initiated by CD8 T cells and requires perforin expression (6, 15, 20, 28). Additionally, a decrease in the BBB tight junction protein occludin has been associated with CNS vascular permeability in the PIFS model (28), the EAE model (8), and the lipopolysaccharide (LPS) injection model of CNS vascular permeability (10, 54). Our laboratory has also demonstrated that a blockade of VEGF preserves the BBB tight junction protein occludin, reduces CNS vascular permeability, and promotes survival (20). In situ mRNA analysis revealed that neurons are the major cellular source of VEGF expression (20). In parallel studies, we also determined that CD8 T cells actively engage Theiler's virus-infected neurons (55). Based on the results of these studies, we propose a direct hypothesis for BBB disruption in which CD8 T cells engage neurons to promote upregulation of VEGF, resulting in disruption of the tight junction architecture and ensuing CNS vascular permeability. Our alternative hypothesis is that CD8 T cells may engage a different CNS cell type to promote vascular permeability through a mechanism that is dependent or independent of neuronally-expressed VEGF. Both the direct and indirect hypotheses require perforin expression.

Other experimental model systems, including LCMV infection, have proposed that monocytic cells and neutrophils are the critical blood-derived cell types promoting BBB disruption. These studies showed that treatment with anti-GR-1 mAb RB6-8C5 extended survival and preserved vascular integrity (13). It was therefore concluded that rather than directly initiating CNS vascular permeability, CD8 T cells may serve to attract other effector populations such as neutrophils to induce damage (13). However, as shown in the results of this study, as well as in previously published results, treatment with anti-GR-1 mAb RB6-8C5 does not specifically deplete neutrophils. (25–27, 29). Importantly, this method results in wide ablation of large numbers of activated CD8 T cells in addition to neutrophils, resulting in preservation of the BBB tight junction proteins and reduced CNS vascular permeability. Meanwhile, treatment with the more neutrophil-specific mAb 1A8 preserved CNS-infiltrating D^b:VP2*121-130* epitope-specific CD8 T cell populations and resulted in disruption of BBB tight junction proteins, extensive CNS vascular permeability, and functional deficit. The difference in the effects of these two mAb treatments requires identification of the immune cell types depleted. We have evaluated GR-1 positivity on other brain-infiltrating cells and found that the vast majority of CD3+ T cells, CD11c+ dendritic cells, and Mac-1+ cells are positive for GR-1 protein. Approximately half of CD4+ T cells and a quarter of NK1.1+ cells are also positive for GR-1 protein. It is therefore likely that a proportion of these GR-1+ cells were also depleted by anti-GR-1 treatment with mAb RB6-8C5. Nevertheless, CD8 T cells are highly attenuated by anti-GR-1 treatment with mAb RB6-8C5 and therefore continue to support our central hypothesis that CD8 T cell infiltration into the CNS is required for initiation of BBB disruption. The finding that virus-specific CD8 T cells correlate with immunopathology resulting from viral infection is in accordance with other previously published work using the LCMV model (11, 12, 14) and consistent with clinical observations where CD8 T cells are associated with vascular permeability in human disease (56–59).

The results obtained in this study highlight the importance of CD8 T cells in promoting vascular permeability and warrants the re-evaluation of the literature pertaining to the extent neutrophils are required for BBB disruption (13, 34, 35). It remains possible that CD8 T cells could engage multiple CNS cell types to promote CNS vascular permeability, and this is currently under investigation in our laboratory. Nevertheless, the data put forward in this study offer new insight into the extent CD8 T cells contribute to disruption of the BBB in the absence of neutrophil support. Defining the specific immune cell types responsible for BBB disruption is essential in order to develop novel therapeutic approaches for neurological diseases. Therefore, targeting CD8 T cells may hold promise as a therapeutic approach to ameliorate pathology associated with BBB disruption. Another approach may involve targeting VEGF and VEGF-related signaling pathways. VEGF has been associated with increased vascular permeability in both the PIFS model (20) and the EAE model (8). Efforts are under way to evaluate the potential of this approach, as we have previously demonstrated that inhibition of neuropilin-1, a co-receptor for VEGF, caused preservation of occludin protein levels and a reduction in vascular permeability (20). Nevertheless, future research to define additional mechanisms by which immune cells contribute to BBB disruption will continue to aid in the development of potential therapies to treat immune-mediated neurological disorders characterized by extensive CNS vascular permeability.

Acknowledgments

We would like to thank Dr. Slobodan I. Macura and Dr. Prasanna K. Mishra (Mayo Clinic, Rochester, Minnesota) for MRI technical assistance, and Michael J. Hansen (Mayo Clinic, Rochester, MN) for assistance with injections.

This work is supported by the National Institutes of Health grants R01 NS060881 and R01 NS58698.

Abbreviations used in this article

BBB	blood brain barrier
EAE	experimental autoimmune encephalomyelitis
GR-1	granulocyte receptor-1
LCMV	lymphocytic choriomeningitis virus
MRI	magnetic resonance imaging
NRS	normal rat serum
PIFS	peptide induced fatal syndrome
TMEV	Theiler's murine encephalomyelitis virus
VEGF	vascular endothelial growth factor

References

1. Medana IM, Turner GD. Human cerebral malaria and the blood-brain barrier. Int J Parasitol. 2006; 36:555–568. [PubMed: 16616145]
2. Brown H, Hien TT, Day N, Mai NT, Chuong LV, Chau TT, Loc PP, Phu NH, Bethell D, Farrar J, Gatter K, White N, Turner G. Evidence of blood-brain barrier dysfunction in human cerebral malaria. Neuropathol Appl Neurobiol. 1999; 25:331–340. [PubMed: 10476050]
3. Minagar A, Alexander JS. Blood-brain barrier disruption in multiple sclerosis. Mult Scler. 2003; 9:540–549. [PubMed: 14664465]
4. Huber JD, Egleton RD, Davis TP. Molecular physiology and pathophysiology of tight junctions in the blood-brain barrier. Trends Neurosci. 2001; 24:719–725. [PubMed: 11718877]

5. Talavera D, Castillo AM, Dominguez MC, Gutierrez AE, Meza I. IL8 release, tight junction and cytoskeleton dynamic reorganization conducive to permeability increase are induced by dengue virus infection of microvascular endothelial monolayers. The Journal of general virology. 2004; 85:1801–1813. [PubMed: 15218164]
6. Pirko I, Suidan GL, Rodriguez M, Johnson AJ. Acute hemorrhagic demyelination in a murine model of multiple sclerosis. J Neuroinflammation. 2008; 5:31. [PubMed: 18606015]
7. Lacerda-Queiroz N, Rodrigues DH, Vilela MC, Rachid MA, Soriani FM, Sousa LP, Campos RD, Quesniaux VF, Teixeira MM, Teixeira AL. Platelet-activating factor receptor is essential for the development of experimental cerebral malaria. Am J Pathol. 2012; 180:246–255. [PubMed: 22079430]
8. Argaw AT, Gurfein BT, Zhang Y, Zameer A, John GR. VEGF-mediated disruption of endothelial CLN-5 promotes blood-brain barrier breakdown. Proc Natl Acad Sci U S A. 2009; 106:1977–1982. [PubMed: 19174516]
9. Crews FT, Qin LY, Wu XF, Block ML, Liu YX, Bresse GR, Hong JS, Knapp DJ. Systemic LPS causes chronic neuroinflammation and progressive neurodegeneration. Glia. 2007; 55:453–462. [PubMed: 17203472]
10. Brooks TA, Hawkins BT, Huber JD, Egleton RD, Davis TP. Chronic inflammatory pain leads to increased blood-brain barrier permeability and tight junction protein alterations. Am J Physiol Heart Circ Physiol. 2005; 289:H738–743. [PubMed: 15792985]
11. Kagi D, Ledermann B, Burki K, Seiler P, Odermatt B, Olsen KJ, Podack ER, Zinkernagel RM, Hengartner H. Cytotoxicity mediated by T cells and natural killer cells is greatly impaired in perforin-deficient mice. Nature. 1994; 369:31–37. [PubMed: 8164737]
12. Storm P, Bartholdy C, Sorensen MR, Christensen JP, Thomsen AR. Perforin-deficient CD8+ T cells mediate fatal lymphocytic choriomeningitis despite impaired cytokine production. J Virol. 2006; 80:1222–1230. [PubMed: 16414999]
13. Kim JV, Kang SS, Dustin ML, McGavern DB. Myelomonocytic cell recruitment causes fatal CNS vascular injury during acute viral meningitis. Nature. 2009; 457:191–195. [PubMed: 19011611]
14. Matullo CM, Regan KJO, Hensley H, Curtis M, Rall GF. Lymphocytic choriomeningitis virus-induced mortality in mice is triggered by edema and brain herniation. J Virol. 2010; 84:312–320. [PubMed: 19828618]
15. Johnson AJ, Mendez-Fernandez Y, Moyer AM, Sloma CR, Pirko I, Block MS, Rodriguez M, Pease LR. Antigen-specific CD8+ T cells mediate a peptide-induced fatal syndrome. J Immunol. 2005; 174:6854–6862. [PubMed: 15905527]
16. Rodriguez M, Oleszak E, Leibowitz J. Theiler's murine encephalomyelitis: a model of demyelination and persistence of virus. Crit Rev Immunol. 1987; 7:325–365. [PubMed: 2827957]
17. McDole J, Johnson AJ, Pirko I. The role of CD8+ T-cells in lesion formation and axonal dysfunction in multiple sclerosis. Neurol Res. 2006; 28:256–261. [PubMed: 16687050]
18. Johnson AJ, Njenga MK, Hansen MJ, Kuhns ST, Chen L, Rodriguez M, Pease LR. Prevalent class I-restricted T-cell response to the Theiler's virus epitope Db:VP2121-130 in the absence of endogenous CD4 help, tumor necrosis factor alpha, gamma interferon, perforin, or costimulation through CD28. J Virol. 1999; 73:3702–3708. [PubMed: 10196262]
19. Johnson AJ, Upshaw J, Pavelko KD, Rodriguez M, Pease LR. Preservation of motor function by inhibition of CD8+ virus peptide-specific T cells in Theiler's virus infection. Faseb J. 2001; 15:2760–2762. [PubMed: 11606479]
20. Suidan GL, Dickerson JW, Chen Y, McDole JR, Tripathi P, Pirko I, Seroogy KB, Johnson AJ. CD8 T cell-initiated vascular endothelial growth factor expression promotes central nervous system vascular permeability under neuroinflammatory conditions. J Immunol. 2010; 184:1031–1040. [PubMed: 20008293]
21. Gibbs WN, Kreidie MA, Kim RC, Hasso AN. Acute hemorrhagic leukoencephalitis - Neuroimaging features and neuropathologic diagnosis. J Comput Assist Tomo. 2005; 29:689–693.
22. Wong D, Dorovini-Zis K, Vincent SR. Cytokines, nitric oxide, and cGMP modulate the permeability of an in vitro model of the human blood-brain barrier. Exp Neurol. 2004; 190:446–455. [PubMed: 15530883]

23. Tazawa H, Okada F, Kobayashi T, Tada M, Mori Y, Une Y, Sendo F, Kobayashi M, Hosokawa M. Infiltration of neutrophils is required for acquisition of metastatic phenotype of benign murine fibrosarcoma cells: implication of inflammation-associated carcinogenesis and tumor progression. Am J Pathol. 2003; 163:2221–2232. [PubMed: 14633597]
24. Breitbach CJ, Paterson JM, Lemay CG, Falls TJ, McGuire A, Parato KA, Stojdl DF, Daneshmand M, Speth K, Kirn D, McCart JA, Atkins H, Bell JC. Targeted inflammation during oncolytic virus therapy severely compromises tumor blood flow. Mol Ther. 2007; 15:1686–1693. [PubMed: 17579581]
25. Dunay IR, Fuchs A, Sibley LD. Inflammatory monocytes but not neutrophils are necessary to control infection with Toxoplasma gondii in mice. Infection and Immunity. 2010; 78:1564–1570. [PubMed: 20145099]
26. Daley JM, Thomay AA, Connolly MD, Reichner JS, Albina JE. Use of Ly6G-specific monoclonal antibody to deplete neutrophils in mice. J Leukocyte Biol. 2008; 83:64–70. [PubMed: 17884993]
27. Reading PC, Wojtasiak M, Pickett DL, Tate MD, Londrigan SL, Bedoui S, Brooks AG. Depletion of Gr-1(+), but not Ly6G(+), immune cells exacerbates virus replication and disease in an intranasal model of herpes simplex virus type 1 infection. J Gen Virol. 2010; 91:2158–2166. [PubMed: 20538903]
28. Suidan GL, McDole JR, Chen Y, Pirko I, Johnson AJ. Induction of blood brain barrier tight junction protein alterations by CD8 T cells. PLoS One. 2008; 3:e3037. [PubMed: 18725947]
29. Tate MD, Ioannidis LJ, Croker B, Brown LE, Brooks AG, Reading PC. The role of neutrophils during mild and severe influenza virus infections of mice. PLoS One. 2011; 6:e17618. [PubMed: 21423798]
30. Denic A, Macura SI, Mishra P, Gamez JD, Rodriguez M, Pirko I. MRI in rodent models of brain disorders. Neurotherapeutics. 2011; 8:3–18. [PubMed: 21274681]
31. Pirko I, Gamez J, Johnson AJ, Macura SI, Rodriguez M. Dynamics of MRI lesion development in an animal model of viral-induced acute progressive CNS demyelination. Neuroimage. 2004; 21:576–582. [PubMed: 14980559]
32. Pirko I, Johnson AJ, Chen Y, Lindquist DM, Lohrey AK, Ying J, Dunn RS. Brain atrophy correlates with functional outcome in a murine model of multiple sclerosis. Neuroimage. 2011; 54:802–806. [PubMed: 20817104]
33. Pirko I, Nolan TK, Holland SK, Johnson AJ. Multiple sclerosis: pathogenesis and MR imaging features of T1 hypointensities in a [corrected] murine model. Radiology. 2008; 246:790–795. [PubMed: 18309014]
34. Zhou J, Stohlman SA, Hinton DR, Marten NW. Neutrophils promote mononuclear cell infiltration during viral-induced encephalitis. J Immunol. 2003; 170:3331–3336. [PubMed: 12626593]
35. Bolton SJ, Anthony DC, Perry VH. Loss of the tight junction proteins occludin and zonula occludens-1 from cerebral vascular endothelium during neutrophil-induced blood-brain barrier breakdown in vivo. Neuroscience. 1998; 86:1245–1257. [PubMed: 9697130]
36. Robb RA. 3-D visualization in biomedical applications. Annu Rev Biomed Eng. 1999; 1:377–399. [PubMed: 11701494]
37. Robb RA. The biomedical imaging resource at Mayo Clinic. IEEE Trans Med Imaging. 2001; 20:854–867. [PubMed: 11585203]
38. Chen L, Zhang Z, Sendo F. Neutrophils play a critical role in the pathogenesis of experimental cerebral malaria. Clin Exp Immunol. 2000; 120:125–133. [PubMed: 10759773]
39. Melnikov VY, Faubel S, Siegmund B, Lucia MS, Ljubanovic D, Edelstein CL. Neutrophil-independent mechanisms of caspase-1- and IL-18-mediated ischemic acute tubular necrosis in mice. The Journal of clinical investigation. 2002; 110:1083–1091. [PubMed: 12393844]
40. Bliss SK, Gavrilescu LC, Alcaraz A, Denkers EY. Neutrophil depletion during Toxoplasma gondii infection leads to impaired immunity and lethal systemic pathology. Infection and Immunity. 2001; 69:4898–4905. [PubMed: 11447166]
41. Andrews DM, Matthews VB, Sammels LM, Carrello AC, McMinn PC. The severity of murray valley encephalitis in mice is linked to neutrophil infiltration and inducible nitric oxide synthase activity in the central nervous system. J Virol. 1999; 73:8781–8790. [PubMed: 10482632]

42. Cardona AE, Li M, Liu L, Savarin C, Ransohoff RM. Chemokines in and out of the central nervous system: much more than chemotaxis and inflammation. J Leukocyte Biol. 2008; 84:587–594. [PubMed: 18467654]
43. Czuprynski CJ, Brown JF, Maroushek N, Wagner RD, Steinberg H. Administration of anti-granulocyte mAb RB6-8C5 impairs the resistance of mice to Listeria monocytogenes infection. J Immunol. 1994; 152:1836–1846. [PubMed: 8120393]
44. Ingo Bechmann IG, Hugh Perry V. What is the blood-brain barrier (not)? Trends in Immunology. 2007; 28:5–11. [PubMed: 17140851]
45. Burns AR, Bowden RA, MacDonell SD, Walker DC, Odebunmi TO, Donnachie EM, Simon SI, Entman ML, Smith CW. Analysis of tight junctions during neutrophil transendothelial migration. J Cell Sci. 2000; 113:45–57. [PubMed: 10591624]
46. Wolburg H, Wolburg-Buchholz K, Engelhardt B. Diapedesis of mononuclear cells across cerebral venules during experimental autoimmune encephalomyelitis leaves tight junctions intact. Acta Neuropathol. 2005; 109:181–190. [PubMed: 15549331]
47. Zlokovic BV. The blood-brain barrier in health and chronic neurodegenerative disorders. Neuron. 2008; 57:178–201. [PubMed: 18215617]
48. Blamire AM, Anthony DC, Rajagopalan B, Sibson NR, Perry VH, Styles P. Interleukin-1beta -induced changes in blood-brain barrier permeability, apparent diffusion coefficient, and cerebral blood volume in the rat brain: a magnetic resonance study. The Journal of neuroscience : the official journal of the Society for Neuroscience. 2000; 20:8153–8159. [PubMed: 11050138]
49. Ferrari CC, Depino AM, Prada F, Muraro N, Campbell S, Podhajcer O, Perry VH, Anthony DC, Pitossi FJ. Reversible demyelination, blood-brain barrier breakdown, and pronounced neutrophil recruitment induced by chronic IL-1 expression in the brain. American Journal of Pathology. 2004; 165:1827–1837. [PubMed: 15509551]
50. Krizanac-Bengez L, Kapural M, Parkinson F, Cucullo L, Hossain M, Mayberg MR, Janigro D. Effects of transient loss of shear stress on blood-brain barrier endothelium: role of nitric oxide and IL-6. Brain Res. 2003; 977:239–246. [PubMed: 12834884]
51. Laflamme N, Lacroix S, Rivest S. An essential role of interleukin-1beta in mediating NF-kappaB activity and COX-2 transcription in cells of the blood-brain barrier in response to a systemic and localized inflammation but not during endotoxemia. J Neurosci. 1999; 19:10923–10930. [PubMed: 10594073]
52. Paul R, Koedel U, Winkler F, Kieseier BC, Fontana A, Kopf M, Hartung HP, Pfister HW. Lack of IL-6 augments inflammatory response but decreases vascular permeability in bacterial meningitis. Brain. 2003; 126:1873–1882. [PubMed: 12821529]
53. Stoll G, Jander S, Schroeter M. Cytokines in CNS disorders: neurotoxicity versus neuroprotection. J Neural Transm Suppl. 2000; 59:81–89. [PubMed: 10961421]
54. Gurney KJ, Estrada EY, Rosenberg GA. Blood-brain barrier disruption by stromelysin-1 facilitates neutrophil infiltration in neuroinflammation. Neurobiol Dis. 2006; 23:87–96. [PubMed: 16624562]
55. McDole JR, Danzer SC, Pun RY, Chen Y, Johnson HL, Pirko I, Johnson AJ. Rapid formation of extended processes and engagement of Theiler's virus-infected neurons by CNS-infiltrating CD8 T cells. Am J Pathol. 2010; 177:1823–1833. [PubMed: 20813972]
56. Mathew A, Rothman AL. Understanding the contribution of cellular immunity to dengue disease pathogenesis. Immunol Rev. 2008; 225:300–313. [PubMed: 18837790]
57. Stephens HA, Klaythong R, Sirikong M, Vaughn DW, Green S, Kalayanarooj S, Endy TP, Libraty DH, Nisalak A, Innis BL, Rothman AL, Ennis FA, Chandanayingyong D. HLA-A and -B allele associations with secondary dengue virus infections correlate with disease severity and the infecting viral serotype in ethnic Thais. Tissue Antigens. 2002; 60:309–318. [PubMed: 12472660]
58. Mongkolsapaya J, Dejnirattisai W, Xu XN, Vasanawathana S, Tangthawornchaikul N, Chairunsri A, Sawasdivorn S, Duangchinda T, Dong T, Rowland-Jones S, Yenchitsomanus PT, McMichael A, Malasit P, Screaton G. Original antigenic sin and apoptosis in the pathogenesis of dengue hemorrhagic fever. Nat Med. 2003; 9:921–927. [PubMed: 12808447]
59. Zivna I, Green S, Vaughn DW, Kalayanarooj S, Stephens HA, Chandanayingyong D, Nisalak A, Ennis FA, Rothman AL. T cell responses to an HLA-B*07-restricted epitope on the dengue NS3 protein correlate with disease severity. J Immunol. 2002; 168:5959–5965. [PubMed: 12023403]

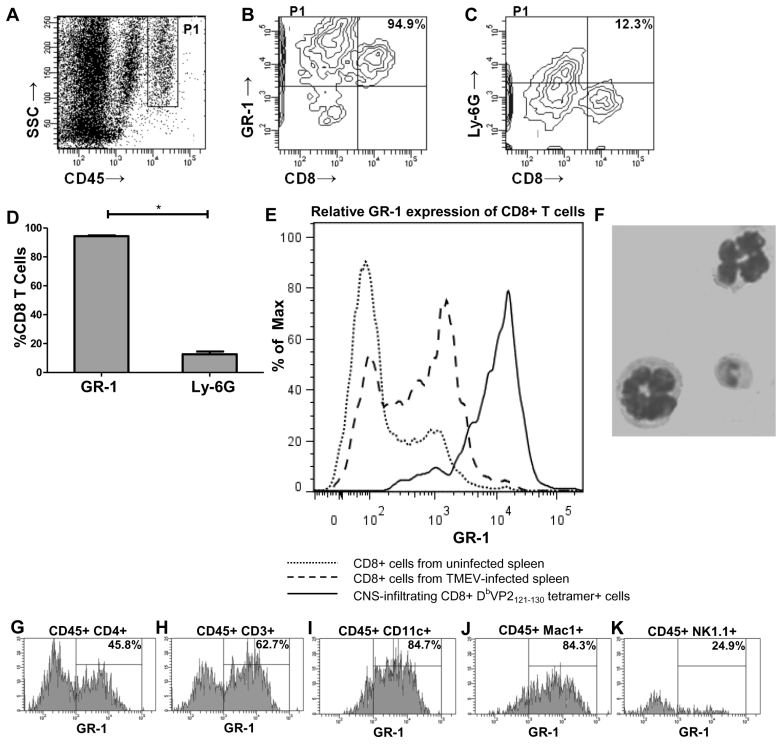

Figure 1. The anti-granulocyte receptor-1 (GR-1) mAb RB6-8C5 binds to CD8+ cells

Contour plots from a representative TMEV-infected C57BL/6 mouse administered $VP2_{121-130}$ peptide to induce PIFS (n=8). (A) The $CD45^{hi}$ population was gated and analyzed for the percentage of CD8+ cells that also express GR-1 or Ly-6G. (B) The majority of brain-infiltrating CD8 T cells also stain positive for GR-1 protein. (C) The vast majority of CD8 T cells are negative for Ly-6G protein. (D) Bar graph showing the significant difference in the percentage of brain-infiltrating CD8+ cells that express either GR-1 or Ly-6G protein ($p<0.001$ by Student's t-test). Error bars indicate standard error of the mean (SEM). Shown are the results of one experiment representative of two. (E) CNS-infiltrating $D^bVP2_{121-130}$ epitope-specific CD8+ cells isolated from TMEV-infected C57BL/6 mice administered $VP2_{121-130}$ peptide to induce PIFS (n=8) express high levels of GR-1 protein when compared to CD8+ cells isolated from the spleen of uninfected (n=3) ($p<0.001$ by Student's t-test) or intracranially TMEV-infected (n=6) ($p<0.001$ by Student's t-test) C57BL/6 mice. (F) Magnetically sorted brain-infiltrating Ly-6G+ cells have morphological features consistent with neutrophils (i.e. segmented nuclei). Brain-infiltrating (G) CD4+, (H) CD3+, (I) CD11c+, (J) Mac-1+, and (K) NK1.1+ cells isolated from TMEV-infected C57BL/6 mice induced to undergo PIFS (n=4) were analyzed as a percentage of $CD45^{hi}$ cells for expression of GR-1 protein. The vast majority of (H) CD3+, (I) CD11c+, and (J) Mac-1+ cells express GR-1 protein, while approximately half of (G) CD4+ cells and a quarter of (K) NK1.1+ cells express GR-1 protein. Percentages are indicated in the upper right-hand corner of the histograms.

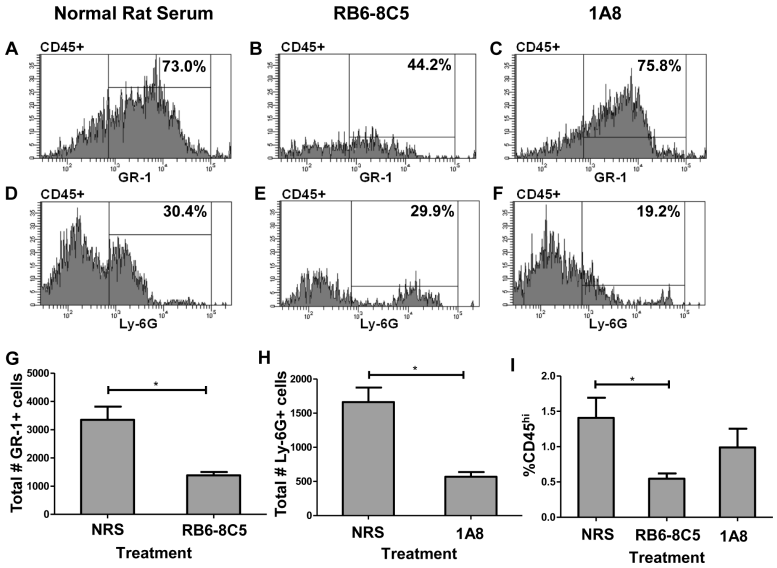

Figure 2. Efficacy of mAb RB6-8C5 and 1A8 neutrophil depletion strategies during acute TMEV infection

Histograms showing the efficacy of neutrophil depletion strategies in representative 7-day TMEV-infected C57BL/6 mice (n=6 per group) using (A,D) normal rat serum, (B,E) RB6-8C5, or (C,F) 1A8. Neutrophil depletion antibodies were administered on days 5, 6, and 7 post-TMEV infection. The $CD45^{hi}$ population was gated and analyzed for the percentages of either GR-1+ or Ly-6G+ cells. (B) RB6-8C5 significantly depleted GR-1+ cells ($p<0.001$ by Student's t-test), and (F) 1A8 significantly depleted Ly-6G+ cells ($p<0.001$ by Student's t-test). (G) RB6-8C5 also significantly depleted the total number of GR-1+ cells per 100,000 events ($p=0.004$ by Mann-Whitney Rank Sum test), and (H) 1A8 significantly depleted the total number of Ly-6G+ cells per 100,000 events ($p=0.002$ by Mann-Whitney Rank Sum test). (I) RB6-8C5 also caused a significant reduction in CD45+ cells as a percentage of whole brain cells when compared to positive controls treated with normal rat serum ($p=0.009$ by Student's t-test). Error bars indicate SEM. Shown in A–F are the results of a representative animal in one experiment of two conducted.

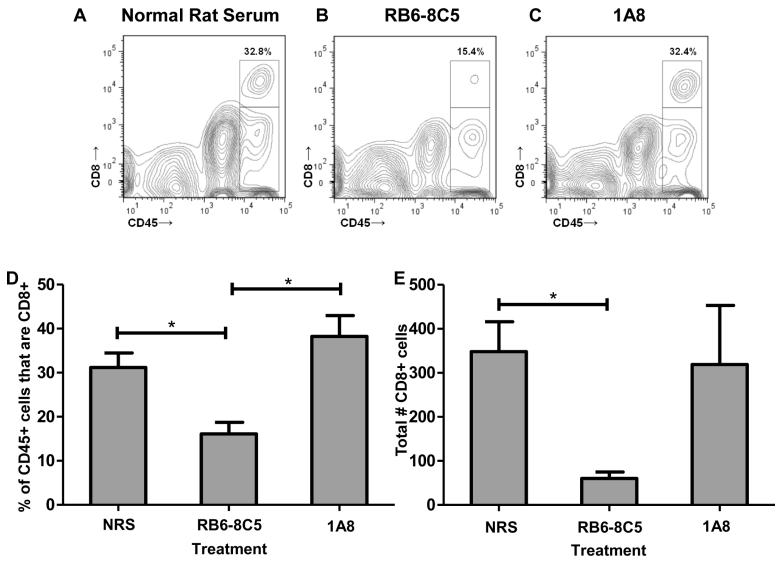

Figure 3. The anti-granulocyte receptor-1 (GR-1) mAb RB6-8C5 depletes CNS-infiltrating CD8+ cells in mice administered $VP2_{121-130}$ peptide to induce PIFS

Representative contour plots showing the effect of treatment with (A) normal rat serum, (B) RB6-8C5, and (C) 1A8 on the percentage of CD45+ cells that are also CD8+. (D) The $CD45^{hi}$ population was gated and analyzed for the percentage of CD8+ cells in each of the three treatment groups (n=6 per group). RB6-8C5-treated mice demonstrated a significant reduction in brain-infiltrating CD8+ cells as a percentage of CD45+ cells when compared to those treated with normal rat serum ($p<0.05$) or 1A8 ($p<0.05$). There was no significant difference between treatment with normal rat serum and treatment with 1A8 ($p=0.386$). (E) Treatment with RB6-8C5 also significantly reduced the total number of CD8+ cells when compared to treatment with normal rat serum ($p<0.05$). Significance between groups was determined by an ANOVA followed by Tukey's multiple comparison test. Error bars indicate SEM. Shown are the results of one experiment representative of two.

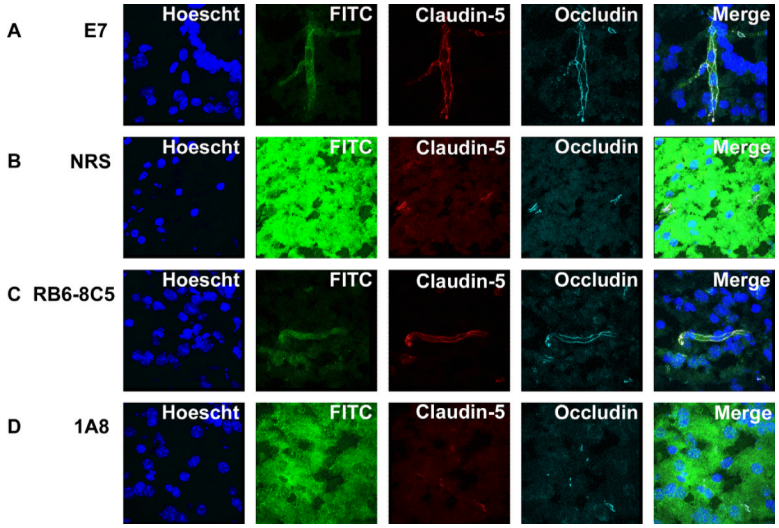

Figure 4. Neutrophil depletion with mAb 1A8 does not preserve BBB tight junctions in CD8 T cell-initiated BBB disruption

Confocal microscopic images from (A) a representative negative control 7-day TMEV-infected C57BL/6 mouse administered mock E7 peptide depict a preservation of vascular integrity and intact tight junction proteins claudin-5 and occludin. (B) Treatment with normal rat serum or (D) depletion of neutrophils with 1A8 mAb treatment is ineffective in reducing degradation of the BBB tight junction proteins claudin-5 and occludin in areas of vascular permeability, as seen through FITC-albumin leakage. Mice treated with (C) RB6-8C5 display a preservation of vascular integrity and intact tight junction proteins on microvessels. Shown are representative images from each of the treatment groups (n=3 per group).

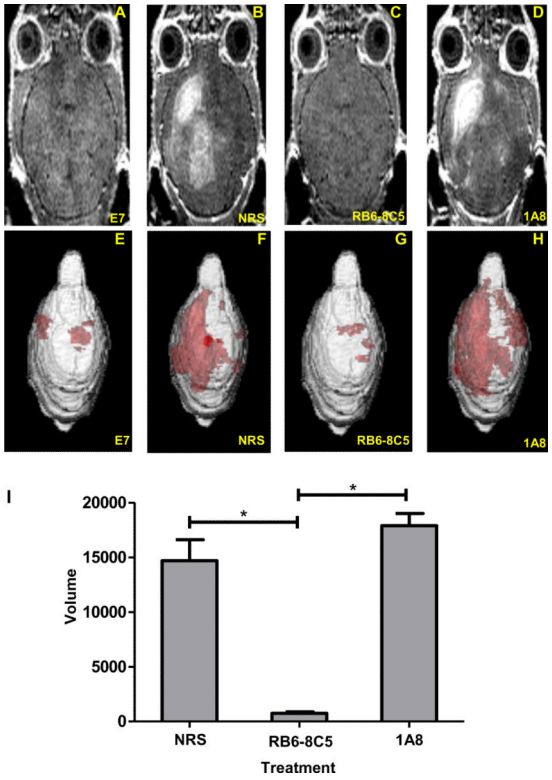

Figure 5. Neutrophil depletion with mAb 1A8 does not preserve vascular integrity as measured by 3D volumetric analysis of gadolinium enhancement visible on T1 weighted MRI

Gadolinium enhanced T1 weighted MRI images showing the extent of vascular permeability in a representative (A) 7-day TMEV-infected mock E7 peptide administered C57BL/6 mouse not undergoing PIFS. In B–D, C57BL/6 mice undergoing PIFS were treated with (B) normal rat serum, (C) RB6-8C5, or (D) 1A8. E–H show 3D transparency rendering of gadolinium enhancing areas generated in Analyze 10.0 in the same animals. Red areas represent subvolumes with gadolinium enhancement. The intensity of red areas is influenced by the overall thickness of underlying gadolinium enhancing volume and by distance from surface. (I) Quantification of the 3D volume of vascular permeability in each of the 3 treatment groups. Treatment with anti-GR-1 mAb RB6-8C5 (n=5) significantly reduced vascular permeability as seen through decreased volumes of gadolinium enhancement when compared to treatment with normal rat serum (n=6) ($p<0.05$) and treatment with anti-Ly-6G mAb 1A8 (n=3) ($p<0.05$). Significance between groups was determined by an ANOVA followed by Dunn's method of multiple comparison. Error bars indicate SEM.

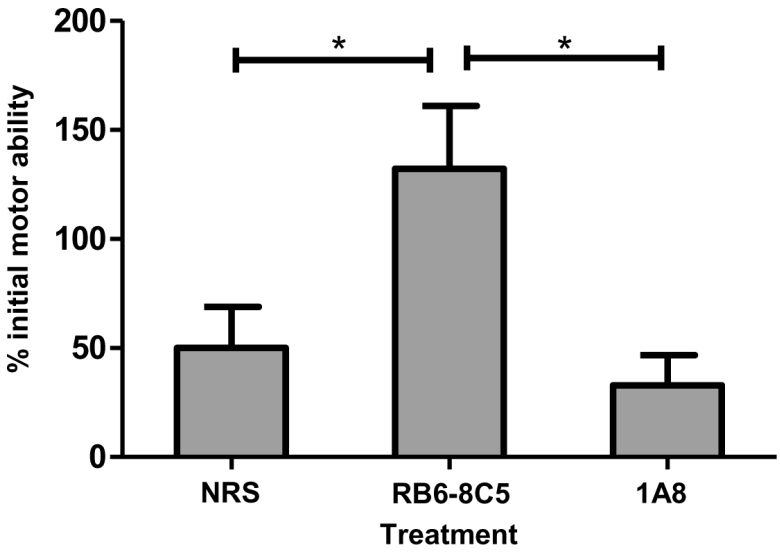

Figure 6. Neutrophil depletion with mAb 1A8 does not preserve functional ability

Mice were assessed on the Rotamex Rotarod before and 24 hours after administration of $VP2_{121-130}$ peptide to initiate PIFS. Scores are depicted as their percent initial rotarod ability prior to induction of PIFS. Treatment with RB6-8C5 (n=10) significantly preserved motor function when compared to treatment with normal rat serum (n=8) ($p<0.05$) and treatment with 1A8 (n=10) ($p<0.05$). There was no significant difference between treatment with normal rat serum and treatment with 1A8 ($p=0.853$). Significance between groups was determined by an ANOVA followed by Tukey's multiple comparison test. Error bars indicate SEM. Shown are the results of one experiment representative of two.